

SOLUTION MINING RESEARCH INSTITUTE

105 Apple Valley Circle
Clarks Summit, PA 18411, USA

Telephone: +1 570-585-8092

Fax: +1 570-585-8091

www.solutionmining.org

Technical
Conference
Paper



**"ADIABATIC" TEMPERATURE CHANGES
IN AN OIL-FILLED CAVERN**

Nicolas Gatelier, GEOSTOCK, Rueil-Malmaison, France

Thierry You, GEOSTOCK, Rueil-Malmaison, France

Pierre Bérest, Ecole Polytechnique, Palaiseau, France

Benoît Brouard, Brouard consulting, Paris, France

SMRI Fall 2008 Technical Conference

13-14 October 2008

Galveston, Texas

“ADIABATIC” TEMPERATURE CHANGES IN AN OIL-FILLED CAVERN

Gatelier Nicolas, You Thierry
GEOSTOCK – 7 rue E. et A. Peugeot, 92563 Rueil-Malmaison, France

Bérest Pierre
LMS, Ecole Polytechnique – Route de Saclay, 91128 Palaiseau, France

Brouard Benoit
Brouard Consulting – 101 rue du Temple, 75003 Paris, France

SUMMARY

Brine warming in a closed cavern generates an increase in brine pressure by approximately 1MPa per °C (80 psi per °F). The inverse also is true: An increase in pressure of any cavern liquid generates instantaneous warming of the liquid followed by gradual cooling, though the cooling starts off quickly for the first couple of weeks. This effect especially is significant in an oil-filled cavern, where a temperature increase of 0.2 °C per MPa (0.26 °F per 100 psi) is typical. In-situ tightness tests performed in an oil storage facility should take this effect into account when a comprehensive interpretation is needed. In this paper, the thermodynamic equations are discussed and an in-situ test performed at the Manosque oil storage, including continuous monitoring of downhole tubing pressure and temperature, is presented as an illustration of this phenomenon.

1. INTRODUCTION

Géostock operates a liquid hydrocarbon storage facility at Manosque (south-eastern France), owned by Géosel-Manosque, in which 26 salt caverns have been leached out since the early 60's. Crude oil, diesel oil, naphtha and kerosene are stored in this facility. The caverns were tested for tightness before commissioning, but it is difficult to perform Mechanical Integrity Tests (MITs) during cavern operation. Nitrogen tests are impossible, as wellheads were not dimensioned to withstand the high gas pressures experienced during a nitrogen-leak MIT. Liquid-liquid MITs are possible; however, due to the large amount of anhydritic blocks embedded in the salt formation, the cavern profiles are not smooth. After hydrocarbons are withdrawn from the cavern — a pre-requisite for an accurate liquid-liquid MIT — small quantities of hydrocarbons trapped in tiny interstices of the rock at the cavern wall are released, making accurate mass-balance determination difficult. For this reason, Géostock designed a test procedure to check for cavern tightness. Ballard and Ehgartner (2000) described a somewhat similar approach (“*CaveMan*”) for pressure analysis and leak detection in an SPR cavern.

Basically, the in-situ test consists of measuring liquid pressure and liquid temperature at cavern depth through accurate downhole gauges, when the cavern is kept idle. When the various phenomena that govern temperature and pressure evolution [(1) transient and steady-state creep closure, (2) brine and oil warming, and (3) additional dissolution generated by pressure and temperature changes] are taken into account, it is possible to infer a value of the (maximum) leak rate. During these tests, the so-called “adiabatic effect” clearly was observed: the rate of the increase in fluid temperature was strongly influenced by the (small) fluid temperature changes triggered by the pressure changes. This must be taken into account when interpreting the results of shut-in tests. This paper is dedicated to this effect. In Section 2, the effects of cavern temperature changes on cavern pressure are recalled and Section 3 is dedicated to the theoretical description of the “*adiabatic*” effects of cavern pressure changes on cavern temperatures. An illustrative example based on data obtained at the Manosque facility is presented in Section 4.

2. THERMAL EXPANSION OF CAVERN LIQUIDS

2.1. Brine warming and thermal expansion

2.1.1. Cavern-liquid warming

Liquids (brine or hydrocarbons) contained in a salt cavern generally are colder than the rock mass surrounding them (Bérest et al., 1979; Ehgartner and Linn, 1994; Van Sambeek et al., 2005). In an idle cavern, cavern liquids gently warm to reach equilibrium with the surrounding rock mass. This process generally is slow —slower still in a larger cavern. A typical example is given in Figure 1. This 300-m deep, 9,000-m³ cavern of the Carresse LPG storage facility operated by Total had been kept idle since 1998. During a test supported by the SMRI, the cavern brine temperature was recorded continuously from June 2002 to October 2002 (Brouard Consulting et al., 2006). The average temperature-increase rate during this period is $\dot{T}_0 = 0.58^\circ\text{C}/\text{yr}$ ($1.04^\circ\text{F}/\text{yr}$), a relatively low figure. Temperature increase rates are much faster in a freshly washed-out cavern, or after a significant change in cavern temperature generated by a large injection of cold fluid.

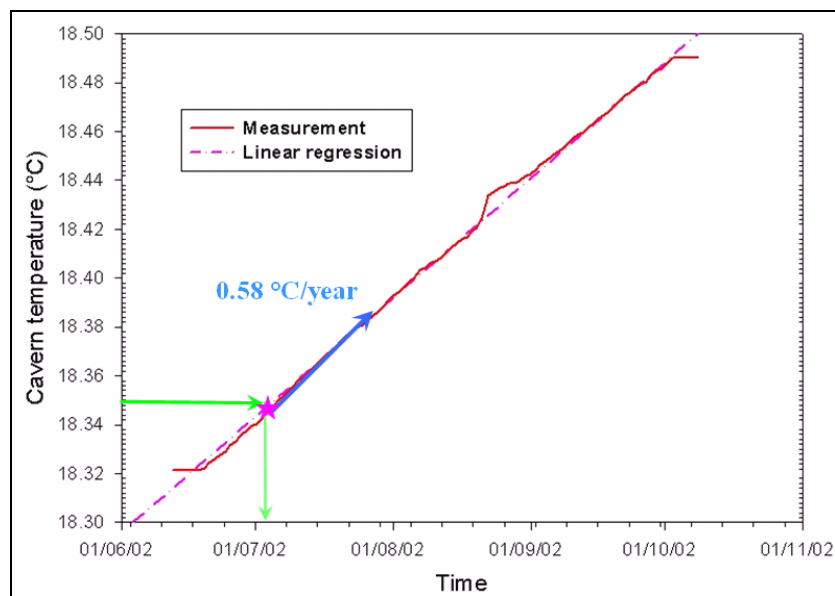


Figure 1. Cavern temperature measurement performed in the SPR2 cavern in 2002.

2.1.2. Cavern-liquid thermal expansion

Brine warming generates brine thermal expansion. The coefficient of brine thermal expansion is $\alpha_b \approx 4.4 \times 10^{-4} / ^\circ\text{C}$ (or $2.4 \times 10^{-4} / ^\circ\text{F}$). In a $V = 100,000 \text{ m}^3$ (600,000 bbls) brine-filled opened cavern, a temperature increase rate of $\dot{T} = 1^\circ\text{C}/\text{yr}$ generates an increase in brine volume by $\dot{V}_b \approx 44 \text{ m}^3/\text{yr}$ (265 bbls/yr). The coefficient of oil thermal expansion is larger, $\alpha_o = 8\text{-}10 \times 10^{-4} / ^\circ\text{C}$ (or $5 \times 10^{-4} / ^\circ\text{F}$); in an oil-filled opened cavern, the oil volume increase would be $\dot{V}_o \approx 100 \text{ m}^3/\text{yr}$ (600 bbls/yr).

2.1.3. Pressure build-up due to thermal expansion

When a cavern is shut-in, free thermal expansion is prevented, and the brine pressure increases as a consequence of brine warming. Let β (in MPa^{-1} , or psi^{-1}) be the cavern compressibility factor (βV , in m^3/MPa or bbls/psi , is the cavern compressibility, which can be measured conveniently by injecting some liquid into the cavern and recording the subsequent pressure build-up, a test often performed at the beginning of an MIT). A typical value is $\beta = 4\text{-}5 \times 10^{-4} / \text{MPa}$ ($3\text{-}4 \times 10^{-6} / \text{psi}$) for a brine-filled cavern and

$\beta = 8\text{-}10 \times 10^{-4} / \text{MPa}$ ($6\text{-}8 \times 10^{-6} \text{ psi}^{-1}$) for an oil-filled cavern. (For a comprehensive discussion, see Bérest et al., 1999.)

In fact, a precise definition of the compressibility factor is not made easily. Additional comments are provided in Appendix B. Here, the compressibility factor is the ratio between the injected liquid flow rate, Q , and the subsequent pressure build-up rate, \dot{P} , divided by cavern volume, or $\beta = Q / V\dot{P}$, as observed *during a rapid injection* (typically, less than one hour long.)

When the cavern is kept idle, the temperature increase rate after several years can be a couple of °C per year or less. However, in a closed and tight cavern, such a slow rate can have significant effects, because an increase rate of $\dot{T} = 1^\circ\text{C}/\text{yr}$ generates a pressure build-up rate of $\dot{P} = \alpha_b \dot{T} / \beta \approx 1 \text{ MPa}/\text{yr}$ (An increase rate of $\dot{T} = 1^\circ\text{F}/\text{yr}$ generates a pressure build-up rate of $\dot{P} \approx 80 \text{ psi}/\text{yr}$.) Magnitudes of the pressure build-up rates are quite similar in an oil-filled cavern and in a brine-filled cavern.

2.2. The consequences of brine warming for shut-in and MITs

2.2.1. Brine warming and shut-in tests

Shut-in tests sometimes are used to calibrate the parameters of a mechanical constitutive model (Brouard et al., 2006). Pressure is monitored for a several-month-long period, and mechanical parameters are back-calculated (through finite-element model computations) to reach a good match between the measured and simulated pressurization rates. However such a method can over-predict the ability of salt to creep when thermal effects are disregarded. In fact, both cavern creep closure and brine thermal expansion contribute to pressurization. A typical creep-closure rate for a 1000-m deep brine-filled cavern is $\dot{V}/V = -3 \times 10^{-4} / \text{yr}$. Creep closure in a shut-in cavern generates pressure build-up by $\dot{P} = -\dot{V} / \beta V$ or, when $\beta = 4 \times 10^{-4} / \text{MPa}$, $\dot{P} = 0.75 \text{ MPa}/\text{yr}$ or $105 \text{ psi}/\text{yr}$ (less in an oil-filled cavern). A relatively slow temperature rise rate, say $\dot{T}_0 = 0.75^\circ\text{C}/\text{yr}$ or $1.35^\circ\text{F}/\text{yr}$, generates a similar pressure build-up rate. For this reason, during a shut-in pressure test, the temperature rise rate must be measured and assessed carefully, and its effects must be subtracted from the as-measured pressure build-up rate to evaluate the creep closure rate correctly.

2.2.2. Brine warming and MITs

The same can be said of an MIT in a large cavern. The leak rate often is inferred from the cavern pressure evolution (\dot{P} , in MPa/day or psi/day), as measured during a so-called liquid-liquid MIT (Van Sambeek et al., 2005), and from the cavern compressibility (βV), as measured at the beginning of the test. The leak rate is deemed to be $Q_{leak} = -\beta V \dot{P}$ (see, for instance, Thiel and Russel, 2004). However, thermal expansion of the brine partly hides the actual leak, as pressure evolution is governed by both leaks and thermal expansion, $\dot{P} = -Q_{leak} / \beta V + \alpha_l \dot{T}_0 / \beta$. Consider, for instance, a relatively large cavern, $V = 500,000 \text{ m}^3$ or $3,000,000 \text{ bbls}$, whose compressibility factor is $\beta = 4 \times 10^{-4} / \text{MPa}$; a leak rate of $Q_{leak} = 500 \text{ bbls}/\text{yr}$ ($80 \text{ m}^3/\text{yr}$) generates a pressure decrease rate of $\dot{P} = -Q_{leak} / \beta V = -0.4 \text{ MPa}/\text{yr}$, but even a relatively slow temperature rise rate, say a few tenths of a °C/yr, hides the effect of the leak, resulting in no or small pressure changes — even when the cavern actually is leaky. (Other phenomena also play roles; a comprehensive review can be found in Van Sambeek et al., 2005).

3. TEMPERATURE CHANGES GENERATED BY PRESSURE CHANGES

3.1. “Adiabatic” temperature changes

In Section 2.1.3 , it was noted that temperature changes in a closed cavern generate pressure changes through brine thermal expansion. To a smaller extent, the inverse also is true. When pressure is built-up rapidly in a closed cavern (say, by injecting liquids into the cavern), the cavern fluid experiences an instantaneous temperature increase by (see Section A.3):

$$\dot{T} = \frac{\alpha_l T}{\rho_l C_l} \dot{P} \quad (1)$$

where $\rho_l C_l$ (in $\text{J/m}^3\text{-}^\circ\text{C}$) is the volumetric heat capacity of the liquid, and T (in Kelvin) is the (absolute) temperature. This effect is termed “*adiabatic*”, as the temperature increase does not result from heat transfer. (During a rapid pressure build-up, no time is left for heat to be transferred from the rock mass to the cavern fluid through the cavern walls.)

Equation (1) can be integrated with respect to time, $\text{Log}[(T_0 + \Delta T_0)/T_0] = (\alpha_l / \rho_l C_l) \Delta P_0$; however, in most cases, the relative temperature increase is small and

$$\Delta T_0 \approx \frac{\alpha_l T_0}{\rho_l C_l} \Delta P_0 \quad (2)$$

3.2. Magnitude of the “adiabatic” effect

The “adiabatic” effect is more significant in an oil-filled cavern than in a brine-filled cavern. Even if small, the “adiabatic” effect has several important practical consequences. Two examples are discussed in Section 3.3.

Assume, for instance, $T = 300 \text{ K}$ (27°C , or 67.5°F).

- In the case of a brine-filled cavern, $\alpha_b = 4.4 \times 10^{-4} / ^\circ\text{C}$, $\rho_b C_b = 4.6 \times 10^6 \text{ J/m}^3\text{-}^\circ\text{C}$ and $\dot{T}/\dot{P} \approx 3 \times 10^{-2} \text{ }^\circ\text{C/MPa}$: a 1-MPa pressure increase generates a $3 \times 10^{-2} \text{ }^\circ\text{C}$ temperature increase. (A 100-psi pressure increase generates a $0.04 \text{ }^\circ\text{F}$ temperature increase.)
- In the case of an oil-filled cavern, $\alpha_o = 9 \times 10^{-4} / ^\circ\text{C}$, $\rho_o C_o = 1.8 \times 10^6 \text{ J/m}^3\text{-}^\circ\text{C}$ are typical and $\dot{T}/\dot{P} \approx 0.2 \text{ }^\circ\text{C/MPa}$: a 1-MPa pressure increase generates a $0.2 \text{ }^\circ\text{C}$ temperature increase. (A 100-psi pressure increase generates a $0.26 \text{ }^\circ\text{F}$ temperature increase.)

Table 1. Cavern temperature increase generated by a cavern pressure increase

	$^\circ\text{C/MPa}$	$^\circ\text{F/100 psi}$
Brine-filled cavern	0.03	0.04
Oil-filled cavern	0.2	0.26

This *adiabatic temperature increase* is small, but it is followed by a rapid temperature decrease, and the pre-existing *temperature increase rate* due to heat transfer is modified significantly.

3.3. Temperature evolution in a closed cavern

A shut-in test is performed in a closed cavern. Pressure and temperature gauges are set at depth in the cavern. It is assumed that the cavern was kept idle before the test: cavern pressure, or P_0 , was constant, and the “pre-existing” temperature evolution was $T_0 = T_0(t)$; the pre-existing temperature rise rate was $\dot{T}_0 = \dot{T}_0(t)$.

When pressure is increased rapidly at time $t = 0$ by ΔP^0 , the liquid temperature increases from T_0 to $T_0 + \frac{\alpha_l T_0}{\rho_l C_l} \Delta P^0$. The additional temperature increase, or $\Delta T^0 = \frac{\alpha_l T_0}{\rho_l C_l} \Delta P^0$, in general is small. (However, it is larger in an oil-filled cavern than in a brine-filled cavern.) This additional temperature increase slowly resorbs with time. When it is assumed that cavern pressure, or $P_0 + \Delta P^0$, is kept constant for any $t > 0$, additional temperature evolution can be described as follows (see Section C.1):

$$\Delta T(t) = \Delta T^0 f(t) \quad (3)$$

Immediately after the rapid pressure build-up, $f(0) = 1$; after a very long period of time, $f(t)$ vanishes to zero, and $f(\infty) = 0$. The function $f = f(t)$ can be computed numerically for any cavern shape. Because the temperature change, ΔT^0 , generated by the pressure build-up is small, $\Delta T(t)$ also is small. However, the additional temperature rate, $\dot{\Delta T}(t) = \Delta T_0 \dot{f}(t)$, is fast, especially during a couple of weeks or months after the pressure build-up. (It contributes significantly to the “apparent” leak when a liquid-liquid MIT is performed in an oil-filled cavern.) The as-observed temperature rate in the cavern is the sum of the pre-existing temperature rate (\dot{T}_0) plus the additional temperature rate generated by the pressure build-up, $\dot{T} = \dot{T}_0 + \Delta T^0 \dot{f}(t)$: in many cases, the latter is much faster than the former.

In an actual cavern, pressure experiences continuous changes. Any pressure change (whether small or large) generates “adiabatic” temperature changes followed by a slow resorbition of the temperature change. Because the equations that govern adiabatic temperature increase and thermal conduction are linear, all these effects simply can be added (“convoluted”) to compute the overall temperature evolution. An example is described in the next section.

3.4. Example

Consider an idealized spherical salt cavern (see Section C.2) whose volume is $V = 4200 \text{ m}^3$. Oil is stored, and the ratio between the volumetric heat capacity of the salt and the volumetric heat capacity of the oil is $\chi = \rho_{\text{salt}} C_{\text{salt}} / \rho_b C_b = 1.1$. The pre-existing temperature increase rate is $\dot{T}_0 = 1 \text{ }^\circ\text{C/yr}$. At time $t_0 = 0.25 \text{ yr}$, pressure suddenly is increased by $\Delta P^0 = 5 \text{ MPa}$, and the oil temperature increases accordingly by $\Delta T^0 = \alpha_o T \Delta P^0 / \rho_o C_o \approx 0.78 \text{ }^\circ\text{C}$ (see Section 3.2; $\alpha_o = 8.65 \times 10^{-4} / \text{ }^\circ\text{C}$ and $\rho_o C_o = 1.7 \times 10^6 \text{ J/m}^3 \cdot \text{ }^\circ\text{C}$ were selected). Three months later, the cavern pressure is lowered by $-\Delta P^0 = -5 \text{ MPa}$, and the temperature decreases accordingly by $\Delta T^0 \approx -0.78 \text{ }^\circ\text{C}$. As displayed on Figure 2, the temperature rate is deeply influenced by pressure changes. It was $1 \text{ }^\circ\text{C/yr}$ before the test and faster than $10 \text{ }^\circ\text{C/yr}$ during a couple of weeks following the initial pressure build-up performed at t_0 .

When the adiabatic effect is disregarded in an oil-filled cavern, the temperature rate is dramatically overestimated after a pressure build-up and it is underestimated after a pressure release.

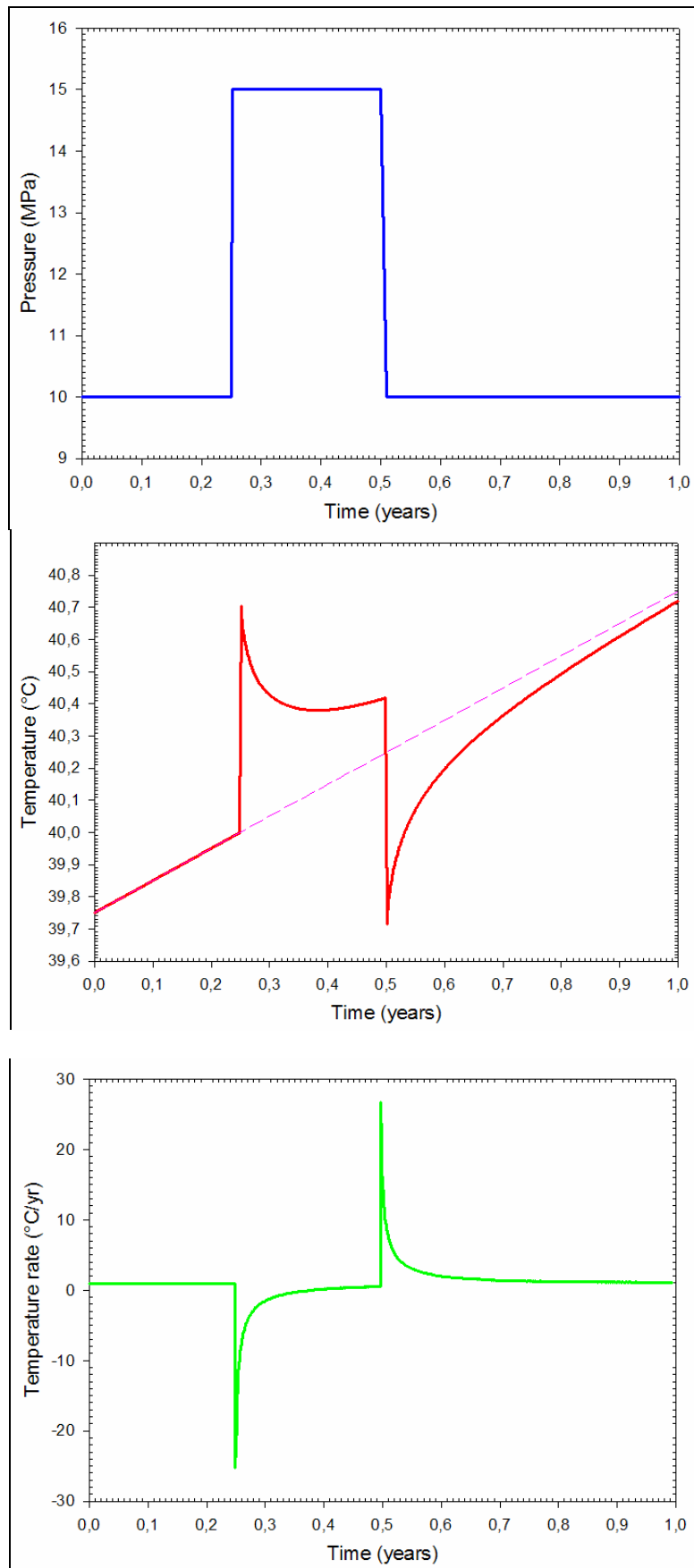


Figure 2. Temperature evolution during and after a 3-month-long pressure step in an idealized oil-filled spherical cavern.

4. A SHUT-IN TEST, CAVERN J OF THE MANOSQUE CAVERN FIELD

4.1. Introduction

A test was performed on the oil-filled Cavern J in the Manosque cavern field. A sonar survey was run in October 1999, and the sonar volume for Cavern J was 314,000 m³. In fact, the excavated volume was 394,000 m³, the insoluble amount was 15%, and the estimated volume of insolubles sedimented in the cavern sump was 59,000 m³. The bulking factor was 1.5 or so, making the apparent volume of sedimented insolubles 88,500 m³; 29,500 m³ of brine are trapped into the sump. From 2002 to 2005, the 314,000-m³ cavern contained 6500 m³ of brine and 307,500 m³ of oil. Obviously, all these figures are tentative rather than exact — the same can be said of such parameters as compressibility and thermal expansion coefficient, among others, which will be introduced below. For simplicity in the following, it is assumed that the cavern is filled with oil whose volume is $V = 314,000 \text{ m}^3$.

The cavern top is 580-m deep, and the cavern bottom (as measured by the sonar survey) is 870-m deep. Figure 3 provides a vertical cross-section of the cavern, in which Sahara-blend oil is stored. The oil density is $\rho_o = 800\text{-}820 \text{ kg/m}^3$, and the oil compressibility is $\beta_o = 8.5 \pm 0.5 \times 10^{-4} / \text{MPa}$, making the cavern compressibility $\beta = \beta_o + \beta_c \approx 10^{-3} / \text{MPa}$. This last figure is consistent with the as-measured cavern compressibility, $\beta V = 310 \text{ m}^3 / \text{MPa}$.

The testing program was designed to estimate the possible cavern leak rate. Test interpretation is positive in the sense that the cavern has been found to be tight within the estimated resolution, which is $\sim 100 \text{ m}^3 / \text{yr}$. In this paper, we focus on the remarkable temperature variations observed during the different phases of the tests owing to continuous downhole monitoring.

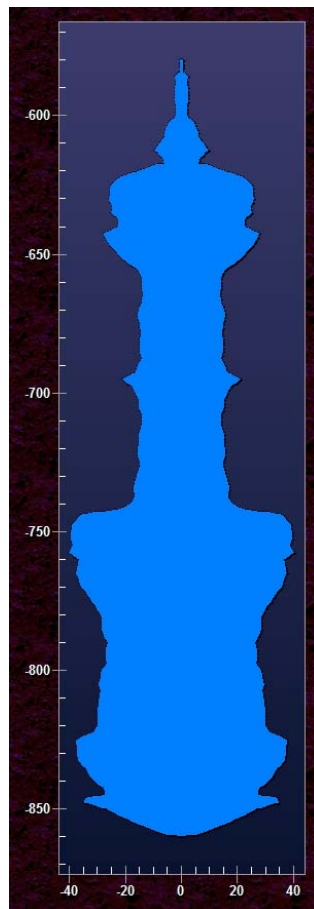


Figure 3. Manosque Cavern J profile.

4.2. Testing program

The cavern was leached out in June 1973 and operated as an oil-storage cavern. The cavern had been kept idle since February 2002. The shut-in test was performed from June 21, 2005 (In the following, this date is the origin of time.) to February 8, 2006 (Day 212). When the test began, the cavern, the central tubing and the annular space were filled with oil. Only a small amount of brine was left at the cavern bottom. A pressure/temperature gauge was lowered into the central tube to a depth of 780 m, where the pressure was approximately $P_0 = 6.2$ MPa.

The testing program was as follows (Figure 4 and Figure 5).

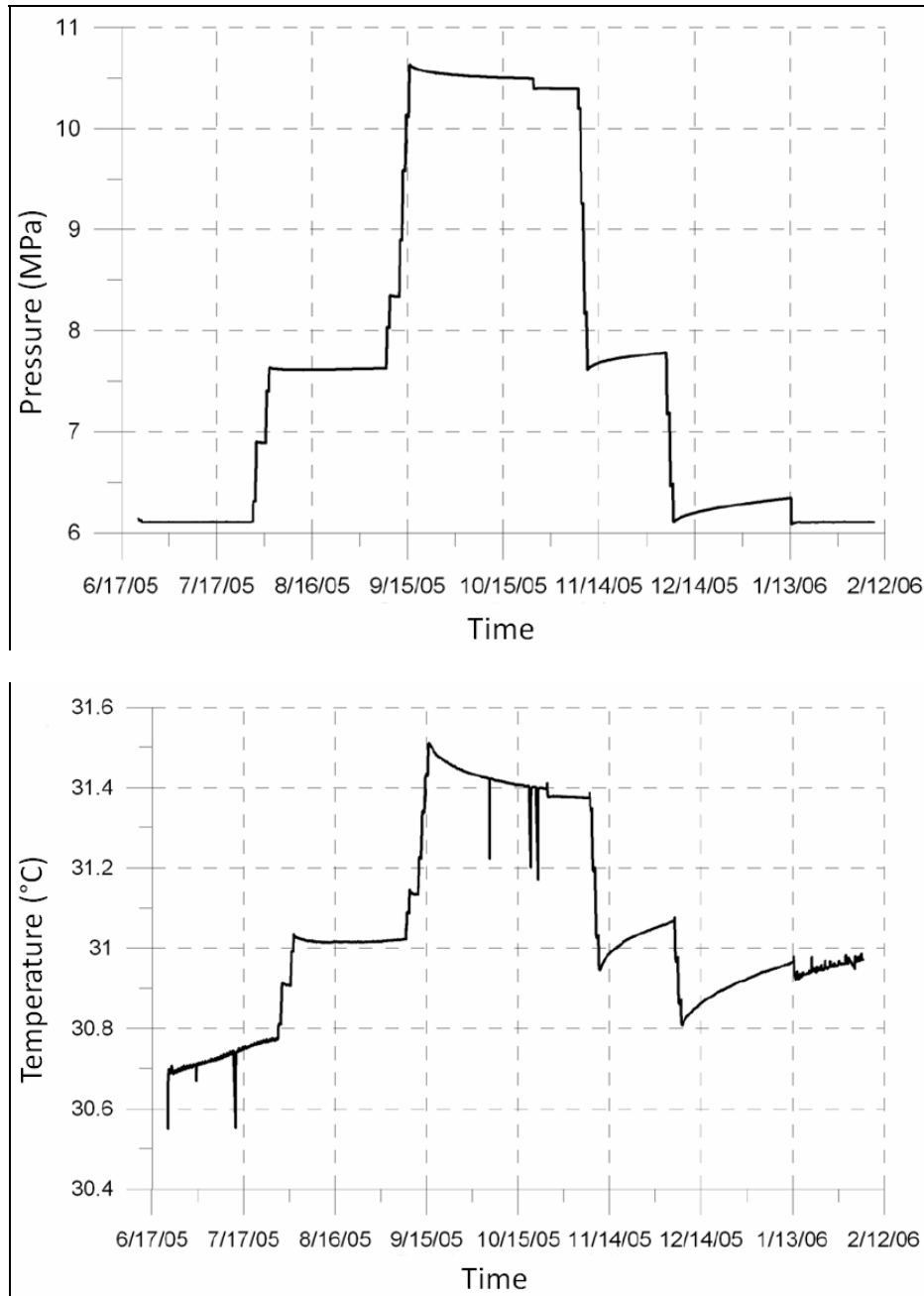


Figure 4. Pressure and temperature evolution June 22, 2005 to February 8, 2006.

Phase 0 — From February 2002 to April 12, 2005, the cavern was kept idle. The annular space was filled with oil, and the tubing was filled with brine. Cavern pressure was halmostatic.

Phase 1 — From April 12 (Day - 80) to April 16 (Day - 76), both the tubing and the annular space were filled with oil and opened to the atmosphere. Cavern pressure decreased by approximately 2.9 MPa.

Phase 2 — The test began on June 21, 2005. From Day 1 to Day 35, the wellhead pressure was kept constant (The wellhead was opened to atmosphere.) A temperature profile log was run (see Section A-2-2), and the cavern temperature was monitored continuously during the entire test. (In hindsight, it would have been slightly better to run the log during Phase 0, as the pressure drop performed during Phase 1 changed the pre-existing temperature evolution.) Cavern pressure at gauge depth (780 m) was 6.2 MPa. The rate of temperature rise during this period is $\dot{T}_0 \approx 0.0025$ °C/day (0.9 °C/yr).

Phase 3 — On Day 35, cavern pressure was increased by 1.5 MPa (cavern pressure 7.7 MPa at gauge depth), and a shut-in test (no injection or withdrawal) was performed for 36 days.

Phase 4 — On Day 71, cavern pressure again was increased by 3 MPa (cavern pressure 10.7 MPa at gauge depth), and a shut-in test was performed for 53 days.

Phase 5 — On Day 126, cavern pressure was lowered by 3 MPa (cavern pressure 7.7 MPa at gauge depth), and a shut-in test was performed for 24 days.

Phase 6 — On Day 150, cavern pressure again was lowered by 1.5 MPa to 6.2 MPa at gauge depth, and a shut-in test was performed for 36 days.

Phase 7 — On Day 186, pressure was lowered to 6.2 MPa at gauge depth; later, wellhead pressure was kept constant for 26 days. At the end of this phase (February 2006), the temperature profile in the well was measured again for comparison with the June 2005 log.

During the pressure increases (or pressure decreases) on Days 35 and 71 (or Days 126 and 150), the cavern temperature increased or decreased accordingly (Figure 4). The ratio between temperature change and pressure change was measured as $\dot{T}/\dot{P} = 0.16$ °C/MPa (0.002 °F/psi). The thermal expansion coefficient of oil is approximately $\alpha_o = 9 \pm 1 \times 10^{-4}$ /°C; the average cavern temperature is $T = 304$ K, and the volumetric heat capacity of the oil is $\rho_o C_o = 1.8 \pm 0.2 \times 10^6$ J/m³-°C. When the average values of these parameters are considered, $\dot{T}/\dot{P} = \alpha_o T / \rho_o C_o = (9 \times 10^{-4})(305) / (1.8 \times 10^6) \approx 0.15$ °C/MPa, a figure that matches the as-measured value. More precise values of these parameters were back-calculated from the numerical computations discussed in the following.

During shut-in phases, cavern pressure experiences significant changes governed by such phenomena as transient and steady-state creep, additional dissolution (a minor contribution, as the cavern is almost completely filled with oil), possible leaks, and oil thermal expansion or contraction. Temperature changes result from the following two phenomena.

1. Pre-existing oil warming — The rate of average temperature rise from June 2005 to February 2006 was inferred from the two temperature profiles: $\dot{T}_0 \approx 0.0025$ °C/day (0.9 °C/yr). However, this rate is not fully representative of the pre-existing temperature rate, as temperature evolution during this period is influenced by the Phase 1 pressure drop. From back-calculations, it was inferred that the pre-existing temperature rate was $\dot{T}_0 \approx 0.5$ °C/yr. From the June 2005 temperature profile log, it also was inferred that the steady-state temperature in the cavern — reached after a very long period of time — should be $T_0(t = \infty) = 36.7$ °C, making the temperature gap in June 2005 equal to 36.7 °C – 30.6 °C = 6.1 °C. To represent the exact temperature history over the 30 years of cavern operation period, a fictitious “initial” temperature gap was back-

calculated (LOCAS software) in order that this fictitious initial gap results in the same rates of temperature and temperature increase as those observed by June 2005.

2. “Adiabatic” temperature changes generated by pressure changes — These temperature changes slowly vanish. Any pressure change by ΔP^0 generates a instantaneous temperature change of $\Delta T^0 = \frac{\alpha_o T}{\rho_o C_o} \Delta P^0$, followed by a slow temperature-change decrease, $\Delta T(t) = \Delta T^0 f(t)$. The function $f = f(t)$ was computed numerically.

Let $P = P(t)$ be the pressure evolution from Day 1 to Day 212. The temperature evolution is

$$T(t) = T_0(t) + \int_0^t \frac{\alpha_l T^0}{\rho_l C_l} \dot{P}(\tau) f(t - \tau) d\tau \quad (4)$$

It is the sum of the pre-existing temperature evolution, or $T_0(t)$, plus the additional temperature change due to cavern pressure changes, or $P(t)$.

This convolution was computed through FEM computations (LOCAS software). The as-measured and the computed evolutions are drawn on Figure 5. The parameters were back-calculated to provide a better fit between the two curves:

$$\rho_{salt} = 2200 \text{ kg/m}^3, C_{salt} = 900 \text{ J/kg-}^\circ\text{C}, \alpha_o = 7.5 \times 10^{-4} /^\circ\text{C}, \beta_o = 7.3 \times 10^{-4} / \text{MPa},$$

$$k_{salt} = 2.63 \times 10^{-6} \text{ m}^2/\text{s}, \rho_o = 803 \text{ kg/m}^3 \text{ (at } 20^\circ\text{C and } 0.1 \text{ MPa)}, C_o = 1700 \text{ J/kg-}^\circ\text{C}.$$

An optimisation procedure should have allowed a still better fit, but the results were considered to be satisfactory.

5. CONCLUSIONS

It has been proven that the “adiabatic” effect (cavern temperature increase generated by cavern pressure increase) is significant, especially in salt caverns filled with liquid or liquefied hydrocarbons. This effect must be taken into account when assessing cavern temperature evolution, an important phenomenon when monitoring cavern tightness.

Actual tests were performed on idle caverns of the Géosel-Manosque storage using a downhole tool for temperature and pressure measurement.

Knowledge of the cavern temperature variation is a fundamental pre-requisite for a comprehensive test interpretation and an accurate assessment of the possible cavern leak rate. The interpretation proposed in this paper takes into account both heat transfer and adiabatic effects; it allows the determination of the basic parameters whose knowledge is required to compute temperature variations when pressure variations are known. Thermo-mechanical evolution of the cavern can then be accurately predicted.

ACKNOWLEDGEMENTS

Special Thanks to K. Sikora and C. Fairhurst. The authors are grateful to Géosel-Manosque which gave permission to publish the data obtained during the cavern J test.

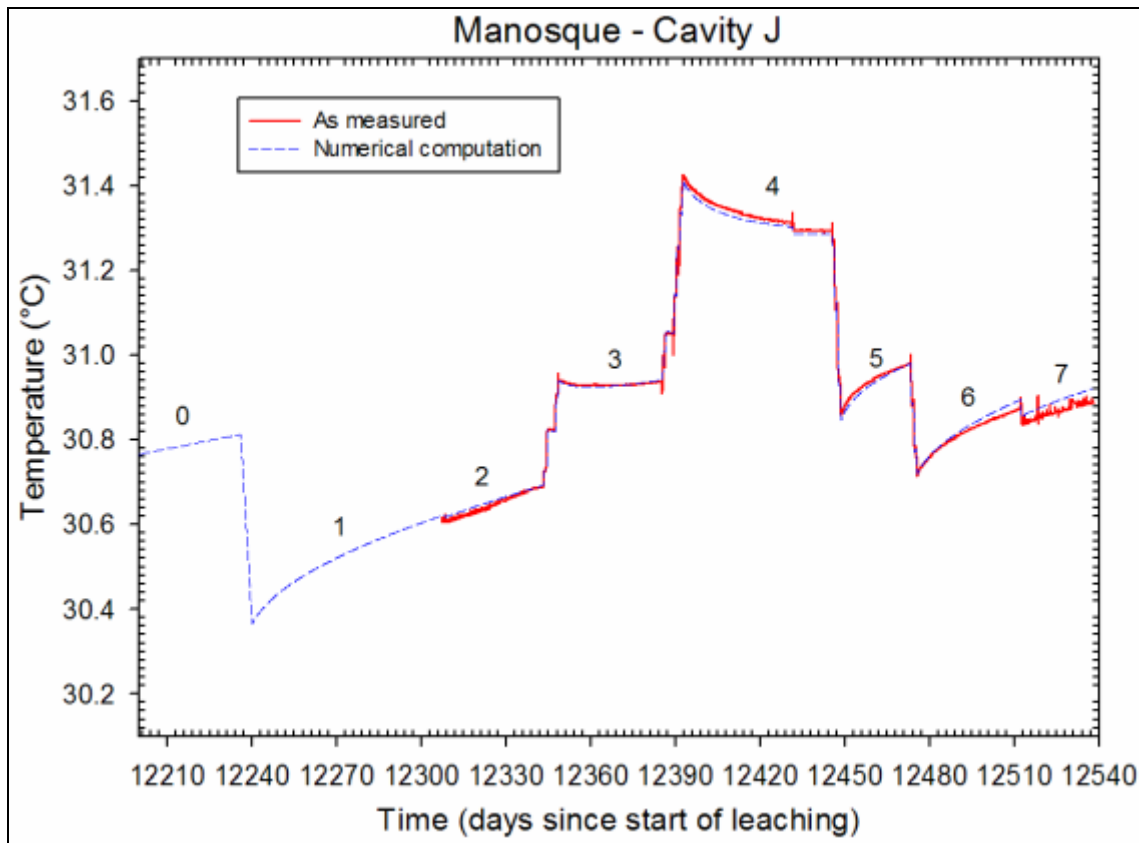


Figure 5 – Numerical simulation of the test.

REFERENCES

- Ballard S. and Ehgartner B.L. (2000). *CaveMan Version 3.0: A Software System for SPR Cavern Pressure Analysis*. Sandia Report SAND2000-1751 Printed July 2000.
- Bérest P., Ledoux E., Legait B. and de Marsily G. (1979). Thermal effects in salt caverns. *Proc. 4th ISRM Congress*. Rotterdam : Balkema, vol. I, 31-35. [in French]
- Bérest P., Bergues J., Brouard B. (1999). Review of static and dynamic compressibility issues relating to deep underground caverns. *Int. J. Rock Mech. Min. Geol. Abstr.* 1999;36:1031-49.
- Brouard Consulting, Institute für Unterirdisches Bauen (IUB), Ecole Polytechnique, Total E&P France, Géostock (2006). *Salt-Cavern Abandonment Field Test in Carresse*. SMRI RFP 2003-2-B, Final Report, April 2006, 98 pages.
- Ehgartner B.L. and Linn J.K. (1994). Mechanical behavior of sealed SPR caverns. *SMRI Spring Meeting*, Houston, Texas.
- Karimi-Jafari M., Brouard B. & Bérest P. (2007). Thermal Effects in Salt Caverns. *Proc. SMRI Spring Meeting*, Basel, Switzerland, 179-190.
- Thiel W.R. and Russel J.M. (2004). Pressure Observation Testing Solution Mined Underground Storage Caverns in Kansas. *Proc. SMRI Spring Meeting*, Wichita, 186-198.
- Van Sambeek L.L., Bérest P. and Brouard B. (2005). *Improvements in Mechanical Integrity Tests for solution-mined caverns used for mineral production or liquid-product storage*. SMRI Research Project Report 2005-1:142 pages.

APPENDIX A. Thermal Effects in a Salt Cavern

In this appendix, the following three issues are discussed:

- (1) a cavern that was kept idle for a very long period of time (Thermal steady-state is reached, and the average temperature of the liquid equals the natural temperature of the rock mass at cavern depth. The cavern is the seat of a perpetual convective flow that stirs the cavern liquid and makes its temperature roughly homogeneous throughout the whole cavern.);
- (2) a cavern under operation (The average liquid temperature generally is colder than the natural temperature of the rock mass at cavern depth. Heat conduction takes place from the rock mass to the cavern, and the liquid slowly warms. However, convection in the cavern liquid also occurs, making the fluid temperatures roughly homogeneous.); and
- (3) a cavern whose pressure is changed suddenly. (The cavern temperature changes accordingly. This change is homogeneous throughout the entire cavern (when the cavern contains a single liquid) and does not modify liquid convection; heat conduction from or to the rock mass is changed. The temperature change is generally small, but the rate of temperature change is significant for several months following the initial rapid pressure build-up.)

A.1. Thermal convection in a fluid-filled cavern

Here, we consider a cavern that has been left idle for a long period of time. (No fluid injection or withdrawal occurs during this period.) At the end of this period, the *average* temperature of cavern fluid equals the *average* rock temperature at cavern depth. However, at a given depth, the fluid temperature can be slightly warmer or colder than the rock temperature, because the brine is stirred perennially by thermal convection (Figure 6 and Figure 7).

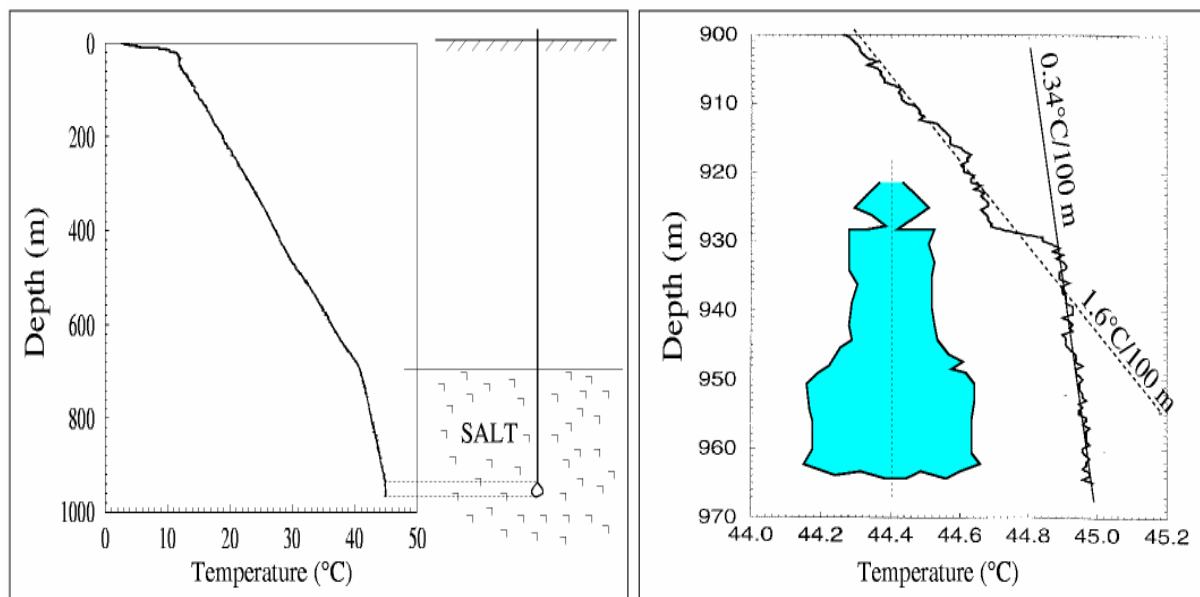


Figure 6. As-measured brine temperature gradient ($0.34\text{ }^{\circ}\text{C/m}$) in the 950-m deep, 8000-m^3 EZ53 cavern operated by Gaz de France is smaller than the rock temperature gradient ($1.6\text{ }^{\circ}\text{C/m}$). This cavern was idle for 14 years before the temperature log was run (Bérest et al., 2001).

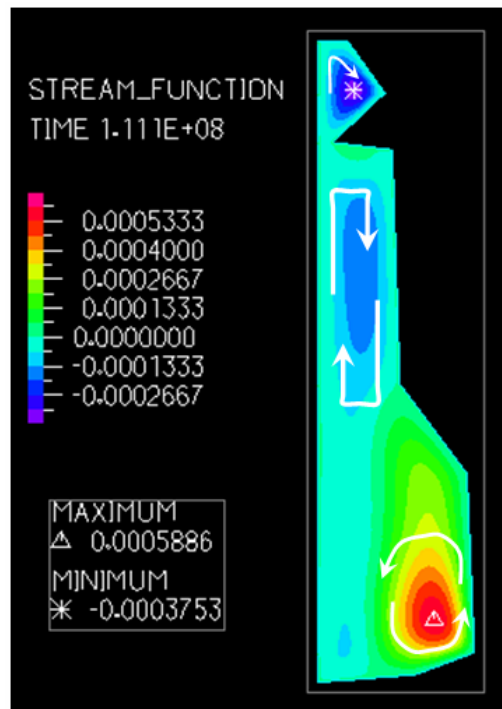


Figure 7. As-computed convection cells in the EZ53 cavern. Axisymmetry of the cells is assumed (Karimi-Jafari et al., 2007).

Rock mass temperature increases with depth. In salt beds or domes, a typical value of the geothermal gradient is $G = 0.016 \text{ }^\circ\text{C/m}$, or $0.009 \text{ }^\circ\text{F/ft}$. In a 500-m (1550-ft) high cavern, the geothermal temperature at the cavern bottom is warmer than the geothermal temperature at the cavern top by $9 \text{ }^\circ\text{C}$ ($16 \text{ }^\circ\text{F}$). Liquid is warmer at the cavern bottom than it is at the cavern top, and its density is smaller. A stable equilibrium is impossible when a heavier liquid overlays a lighter liquid. Driven by gravity forces, the lower (and lighter) liquid rises and is replaced by heavier fluid flowing down. Thus, a set of convection cells is generated in the cavern. Thermal convection stirs the cavern fluid and homogenizes the fluid temperature in the convection cell: the thermal gradient in the cavern is significantly smaller than the geothermal (virgin) gradient. An example of this is given in Figures 5 and 6: the vertical temperature gradient is smaller in the cavern than it is in the well above the cavern, and three convection cells are generated in the cavern brine mass. [Convection flow in the cavern was computed using the “Boussinesq” approximation (Karimi-Jafari et al., 2007).]

When the cavern is filled with saturated brine, things are slightly more complicated, as brine concentration (i.e., the amount of salt that can be dissolved in a given mass of water) is a function of temperature and pressure. Warm brine flows upward and slowly cools; when reaching the cavern top, brine becomes slightly over-saturated (because pressure and temperature are smaller at the cavern top), and crystallisation takes place. Conversely, dissolution occurs at the cavern bottom and, as a whole, the cavern moves down inside the rock mass. Movement is exceedingly slow.

When the cavern is filled partly with liquid hydrocarbons (say, oil), two convection-cell systems develop — in the oil mass and in the brine mass— and heat is exchanged through the oil/brine interface.

A.2. Thermal transient behaviour of a liquid-filled cavern

A.2.1. Thermal conduction in the rock mass

Consider, here, a hydrocarbon storage cavern or a brine production cavern during its operating life-time. The average temperature of the cavern liquid does not equal the average geothermal temperature of the rock at cavern depth, because cold or warm fluids frequently are injected into or withdrawn from the cavern. Cavern fluids generally are colder than the rock mass and gently warm.

For instance, the temperature of a salt mass typically is $T_R = 45^\circ\text{C}$ (113°F) at a $H = 1000\text{ m}$ (3100ft) depth. Caverns are leached using soft water pumped from a river, lake or shallow aquifer whose temperature can be 15°C (59°F). The transit time of leach water in the cavern is a few days (or weeks in a large cavern), and not enough time is provided for circulating water to reach thermal equilibrium with the surrounding rock mass. Brine temperature in the cavern during and at the end of leaching is close to the soft-water temperature and can be colder than the rock temperature by one or several tens of degrees Celsius.

The same can be said of an operating liquid-storage cavern when cold hydrocarbons and warm brine are injected in or withdrawn from the cavern. A precise heat balance is difficult to obtain, as heat also is exchanged in the well between hydrocarbons and brine during injection or withdrawal. In most cases, at the end of an injection phase, the hydrocarbon temperature is significantly colder than the rock temperature at cavern depth.

When the cavern remains idle, after leaching is completed or when no product movement takes place, the initial temperature gap slowly declines with time. Heat is transferred from the surrounding salt mass to the cavern fluids (hydrocarbons and/or brine) whose temperature slowly increases. Fluid temperature ultimately will reach equilibrium with the rock mass and, in the very long term, the cavern temperature will remain constant. The perpetual heat exchange will be governed by steady-state convection in the fluid mass, as described in Section A.1.

A.2.2. Example: Cavern J thermal profile

During the transient phase, when the average fluid temperature still is significantly colder than the geothermal temperature of the rock, convection is also active. Consider, for instance, Cavern J temperature profiles (Figure 8), which were taken in June 2005 and February 2006.

- From 0 to 60 m, the temperature profile in the well is influenced by yearly fluctuations of atmospheric temperature, which is much colder in winter than it is in early summer.
- From 60 to 300 m, the temperature gradient in the well is $4.15^\circ\text{C}/100\text{-m}$, a figure commonly observed in marly formations.
- Below the top of the salt formation (which is 485.6 m deep) and above the cavern roof, the geothermal gradient is $1.7^\circ\text{C}/100\text{ m}$, as commonly observed in salt formations.
- In the cavern itself, from 720 m to 840 m, the cavern oil temperature is significantly smaller than the rock temperature. (Oil warming is a slow process, spread over several years or decades). However, the oil temperature is almost uniform, except at cavern bottom, because the brine-filled sump is warmer than the cavern main body. Note that oil temperature slightly increases by 0.6°C between June 2005 and February 2006 and remains almost uniform throughout the entire cavern.

These observations strongly suggest that the evolution of cavern temperature results from two distinct heat-transfer processes: (1) heat conduction through the rock mass, which results in slow oil warming; and (2) heat convection through the liquid, which results in liquid temperature homogenisation.

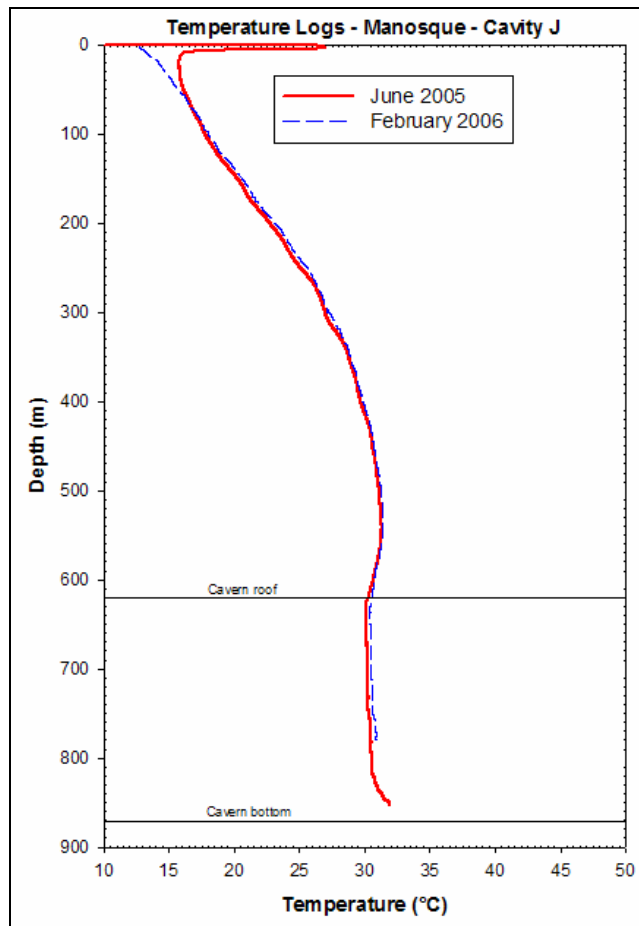


Figure 8. Cavern J temperature profile in June 2005 and February 2006.

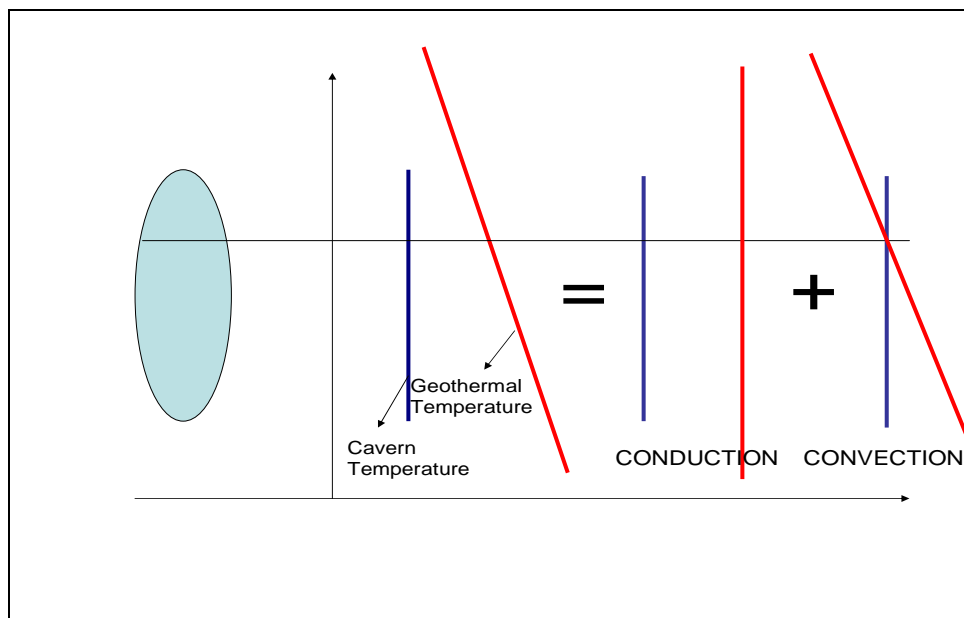


Figure 9. Temperature evolution can be split into two independent processes.

Strictly speaking, these two processes are coupled: the conduction process driven by the temperature unbalance between the cavern and the rock mass certainly influences the convection process in the cavern; and the convection process in the cavern generates heat conduction in the rock mass. (However, the overall heat flux through the cavern walls generated by convection alone is null or small.) The Cavern J

example suggests that, at least when the thermal unbalance is not very large, the actual temperature evolution results from combination of the two mechanisms which, as a first approximation, can be considered to be independent:

- (1) thermal convection, driven by the existence of the geothermal gradient in the rock mass and leading to temperature homogenisation in the cavern. (Steady state is reached rapidly; thermal convection is perpetual (see Section A.1).); and
- (2) thermal conduction, driven by the existence of a difference between the average temperature of the rock mass and the average temperature of the cavern fluid. (What “average temperature of the rock mass” actually means is discussed in Section A.2.3). This process leads to resorption of the temperature unbalance between the rock mass and the cavern fluid, and is transient and slow — several decades long in a large cavern. It comes to an end when the initial thermal balance is resorbed.

In other words (see Figure 9), when computing temperature evolution in an idle cavern, the overall heat transfer process can be split into two parts: (a) the “convection” process, which stirs the cavern liquid and makes its temperature homogeneous; and (b) a “conduction” process, which slowly warms the cavern liquid. The conduction process is described in the next section.

A.2.3. Mathematical description of conduction through the rock mass

Appropriate heat-transfer equations can be written as follows and are explained below.

$$\frac{\partial T_{salt}}{\partial t} = k_{salt} \Delta T_{salt} \quad (\text{A.1})$$

$$T_l(t) = T_{salt} \quad \text{on } \partial\Omega \quad (\text{A.2})$$

$$\rho_l C_l V \dot{T}_l = \int_{\partial\Omega} K_{salt} \frac{\partial T_{salt}}{\partial n} da \quad (\text{A.3})$$

$$T_l(t=0) = T_0 \quad \text{and} \quad T_{salt}(t=0, \underline{x}) = T_{salt}^0(\underline{x}) \quad (\text{A.4})$$

(A.1) This equation holds in the rock mass and describes conductive heat transfer. Δ is the Laplacian operator; T_{salt} is the temperature of the rock mass, which is a function of time and space; k_{salt} is the thermal diffusivity of the salt ($k_{salt} = 3 \times 10^{-6} \text{ m}^2/\text{s} \approx 100 \text{ m}^2/\text{yr}$ is typical). Equation (A.1) is linear: the effects of various thermal loading at different periods are uncoupled and simply can be added. For instance, consider a brine-filled cavern leached out using cold brine. After leaching is completed, brine gently warms to reach thermal equilibrium with the surrounding rock mass. When the cavern pressure suddenly is built up, the brine temperature increases slightly by ΔT^0 (see Section A.3). The effect of this additional temperature change can be discussed using the system (A.1) (A.2) (A.3) and (A.4): $T_l(t=0) = \Delta T_0$ and $T_{salt}(t=0, \underline{x}) = 0$, as temperature changes generated by cavern pressure build-up are independent of the pre-existing warming process, which continues on its own. The two processes can be added to obtain temperature evolution.

(A.2) This equation describes the first boundary condition at the cavern wall ($\partial\Omega$). The fluid temperature of the cavern, or $T_l = T_l(t)$, is uniform through the whole cavern (an assumption supported by the existence of convection in the cavern) and equals the rock temperature at the cavern wall. (No “thermal resistance” is taken into account.)

(A.3) The third equation is the second boundary condition at the cavern wall ($\partial\Omega$). It states that the heat flow crossing through the cavern wall [the right-hand side of (A.3)] is used to warm the cavern fluid [the left-hand side of (A.3)]. K_{salt} is the thermal conductivity of the salt ($K_{salt} = k_{salt} \rho_{salt} C_{salt} = 5\text{-}6 \text{ W/m}\cdot^\circ\text{C}$ is typical; n is the direction of the outward unit vector normal to cavern wall). $\rho_l C_l$ is the volumetric heat capacity of the fluid: for brine, $\rho_b C_b = 4.6 \times 10^6 \text{ J}/^\circ\text{C}\cdot\text{m}^3$; for oil, $\rho_o C_o = 1.8 \times 10^6 \text{ J}/^\circ\text{C}\cdot\text{m}^3$ is typical). However, it must be noted that Equation (A.3) is a simplified version of the energy balance equation, which will be discussed in Section A.3.

(A.4) The last equation describes the initial conditions in the cavern and in the rock mass:

- Rock temperature, or $T_0^{salt}(\infty)$, at large distance from the cavern is the “average” rock temperature. (The geothermal gradient is not considered.) In a tall cavern, the “average” rock temperature is not defined easily: it is not the geothermal temperature at cavern mid-depth. One possible procedure involves computing the final “convective” liquid temperature (obtained by computing the solution of (A.1), (A.2), (A.3) and (A.4) reached after a very long period of time); the “average” rock temperature considered when computing the conductive heat process can be taken as being equal to this long-term liquid temperature.
- These conditions often are difficult to know exactly, as such a cavern may experience many fluid injections and withdrawals, each of them generating temperature changes in the rock mass and in the cavern itself. A simplified procedure sometimes can be used (Brouard et al., 2006): at a given instant, say t_0 , cavern temperature (T_0) and temperature rate (\dot{T}_0) are measured. A fictitious cavern-creation time and a fictitious initial temperature gap between the liquid temperature and the rock temperature at large distance from the cavern (assumed to be uniform through the whole rock mass) are back-calculated such that cavern temperature and temperature rise rate at time t_0 are T_0 and \dot{T}_0 , respectively. This “fictitious” cavern-temperature history generally provides a good match with the actual cavern temperature history.

A.2.4. Characteristic times

It is convenient to re-write Equations (2) and (3) in dimensionless form. Let $t_c = R^2 / \pi k_{salt} \approx V_c^{2/3} / 8k_{salt}$ be the first thermal characteristic time. In this form, R is the “equivalent” cavern radius such that $V = \frac{4}{3} \pi R^3$. (For instance cavern volume is $V = 8,000 \text{ m}^3$, $V^{1/3} = 20 \text{ m}$, $k_{salt} \approx 100 \text{ m}^2/\text{year}$ and $t_c = 0.5 \text{ year}$; in a larger cavern, $V = 512,000 \text{ m}^3$, $V^{1/3} = 80 \text{ m}$ and $t_c = 32 \text{ years}$). In addition, let $\chi = \rho_{salt} C_{salt} / \rho_l C_l$ (for instance, $\rho_{salt} C_{salt} = 2 \times 10^6 \text{ J}/^\circ\text{C}\cdot\text{m}^3$: when the cavern is filled with brine, $\rho_b C_b = 4.6 \times 10^6 \text{ J}/^\circ\text{C}\cdot\text{m}^3$ and $\chi_b \approx 0.42$; when the cavern is filled with oil, $\chi_o = \rho_{salt} C_{salt} / \rho_o C_o = 1.1$ is typical). Equations (2) and (3) provide two characteristic times, t_c and t_c / χ . They are of the same order of magnitude (However, in a gas-filled cavern, $\chi_g = \rho_{salt} C_{salt} / \rho_g C_g$ is large, and the second characteristic time is much shorter than the first: the corresponding warming process is much faster in a gas-filled cavern), and any of these two characteristic times can be selected to assess the duration of the fluid warming process. In the case of a perfectly spherical, brine-filled cavern (discussed in Appendix C), after a period lasting $2\text{-}t_c$, or one year in a $V = 8000 \text{ m}^3$ cavern and 64 years in a $V = 512,000 \text{ m}^3$ cavern, approximately 75% of the initial temperature difference has been resorbed. However, the warming process is faster when oil — instead of brine — is stored in the cavern, because χ_o is larger than χ_b . (because oil heat capacity is smaller than brine heat capacity).

A.3. “Adiabatic” compression or expansion

It has been noted that Equation (A.3) is not perfectly exact. Let $q^* = C_l \dot{T} + h_l \dot{P}$ be the amount of heat received by a unit mass of fluid during a reversible process. During a reversible process, both fluid entropy, S , and fluid enthalpy, H , experience changes:

$$\dot{S} = q^*/T \quad \text{and} \quad \dot{H} = q^* + v_l \dot{P}$$

where $v_l = 1/\rho_l$ is the volume of a unit mass of fluid. \dot{S} and \dot{H} must be two exact differential forms; hence, $h_l = -T \left. \frac{\partial v_l}{\partial T} \right|_p$. As $v_l = v_l^0 (\alpha_l \dot{T} - \beta_l \dot{P})$, $h_l = -\alpha_l T v_l^0$, and the heat-energy balance for the cavern liquid can be written

$$\rho_l C_l V \dot{T} - \alpha_l T V \dot{P} = \int_{\partial\Omega} K_{salt} \frac{\partial T_{salt}}{\partial n} da$$

where α_l is the thermal expansion coefficient of the fluid, and T is the (absolute) temperature. In most cases, the additional term ($\alpha_l T V \dot{P}$) can be neglected (see Equation A.3). However, during rapid evolution (for instance, when cavern pressure is increased at the beginning of an MIT test), the right-hand side of the equation can be neglected (In rapid evolution, not enough time is left for heat transfer from the rock mass to the cavern.), and any pressure change generates a temperature change in the cavern by

$$\dot{T} = \frac{\alpha_l T}{\rho_l C_l} \dot{P}$$

When brine is considered, $\rho_b C_b = 4.6 \times 10^6 \text{ J/}^\circ\text{C}\cdot\text{m}^3$, and $\alpha_b = 4.4 \times 10^{-4} /^\circ\text{C}$. When $T = 300 \text{ K}$ (27°C , or 67°F), $\alpha_b T / \rho_b C_b = 0.029 \text{ MPa/}^\circ\text{C}$. For oil, $\rho_o C_o = 1.8 \times 10^6 \text{ J/}^\circ\text{C}\cdot\text{m}^3$, and $\alpha_o = 9 \times 10^{-4} /^\circ\text{C}$, $\alpha_o T / \rho_o C_o \approx 15 \times 10^{-2} \text{ }^\circ\text{C/MPa} \approx 11 \text{ }^\circ\text{F/psi}$.

When the cavern contains brine *and* liquid hydrocarbons, the same phenomenon takes place in the two liquids, and the two liquids experience distinct temperature changes (smaller in brine than in liquid hydrocarbons).

Before such an “adiabatic” pressure change, thermal equilibrium typically does not exist. Usually, the brine temperature in the cavern is lower than the rock mass temperature, which results in heat flux from the rock mass to the cavern. An additional thermal-equilibrium disturbance is created when the brine temperature increases (for instance) following a pressure change. Because the equations that describe the temperature evolution are linear (see A.2.3), the “old” brine warming process that preceded the pressure change and the “new” cooling process triggered by the pressure increase are uncoupled. They can be discussed and computed independently. The overall temperature evolution can be obtained through superposition of the solution for the “new” cooling process and the solution for the “old” warming process.

APPENDIX B. Cavern Compressibility

B.1. Definitions

Adiabatic cavern compressibility (βV) is the ratio between the volume injected (or withdrawn) in (or from) a fluid-filled cavern and the cavern pressure change, when such phenomena as pre-existing or injection-induced fluid cooling/warming, cavern creep closure, additional salt dissolution, fluid leaks through the well and fluid permeation through the cavern walls can be disregarded — an assumption that is approximately correct when rapid injection is performed. β is the cavern compressibility factor, and V is the cavern volume. Adiabatic compressibility is relatively easy to measure. However, when fluid is injected in the annular space (respectively, in the tubing), pressure must be measured in the tubing (respectively, in the annular space). When extremely precise measurement is needed, the effects of atmospheric pressure variations, ground-level temperature variations, well temperature variations (induced by fluid injection) and pre-existing cavern liquid warming must be taken into account.

Isothermal liquid compressibility factor is a theoretical notion. For instance, when ρ is brine density, T is brine temperature, c is brine concentration, and

$$\dot{\rho} = \rho_0 \left(\beta_b^{isoth} \dot{P} - \alpha_b \dot{T} + \gamma_b \dot{c} \right) \quad (\text{B.1})$$

This quantity cannot be measured directly as, in an actual cavern, neither temperature nor concentration is constant.

The “long-term” compressibility factor is the injected volume/pressure change ratio when additional dissolution is taken into account. It is larger than the adiabatic compressibility factor by approximately 5%.

B.2. Pressure and temperature evolutions during fluid injection

In the following we assume that a flow of fluid (Q , in m^3/hr or bbls/hr) is injected in a closed cavern. Cavern pressure and temperature change rates are \dot{P} and \dot{T} . Cavern volume (V_c), brine volume (V_b) and temperature change rate (\dot{T}) can be described by the following equations:

B.2.1. Cavern volume change

$$\dot{V}_c / V_c = \beta_c \dot{P} - Q_{creep} / V_c + Q_{c,diss} / V_c + \alpha_R \Phi(T_{salt}) \quad (\text{B.2})$$

In a rapid evolution, transient and steady-state cavern creep closure (Q_{creep}) can be disregarded; in most cases, cavern thermal expansion due to changes in rock temperature is exceedingly small, $\Phi = 0$ (Karimi-Jafari et al., 2007); when the fluid contained in the cavern is saturated brine, the cavern volume increase due to additional dissolution ($Q_{c,diss}$) is a function of pressure change and temperature change. It can be disregarded during a rapid evolution, or when the cavern is filled with oil and

$$\dot{V}_c / V_c = \beta_c \dot{P} \quad (\text{B.3})$$

where β_c is a function of the elastic parameters (E, ν) of the rock mass and of the cavern shape.

B.2.2. Liquid volume change

$$\dot{V}_l/V_l = Q/V + \alpha_l \dot{T}_l - \beta_l^{isoth} \dot{P} + Q_{b,diss}/V_l - Q_{leak}/V_l \quad (B.4)$$

Q_{leak} is the (possible) leak rate, and \dot{T}_l (in °C/hr, or °F/hr) is the temperature rise rate, which is the sum of the pre-existing temperature rise rate plus the test-induced temperature rise rate. Increase in cavern volume due to additional dissolution ($Q_{b,diss}$) is a function of pressure change and temperature change. It can be disregarded during a rapid evolution and

$$\dot{V}_l/V_l = (Q - Q_{leak})/V_l + \alpha_l \dot{T}_l - \beta_l^{isoth} \dot{P} \quad (B.5)$$

B.2.3. Cavern temperature change

$$\rho_l C_l V_l \dot{T}_l - \alpha_l T V_l \dot{P} = Q^* \quad (B.6)$$

Because the cavern is assumed to be idle when the test begins, the additional heat flux can be neglected during a rapid increase in pressure. $Q^* = \rho_l C_l V_l \dot{T}_0$ is the heat transferred from the rock mass to the cavern fluid through the cavern walls before the test begins. This heat flux generates a rate of temperature increase of \dot{T}_0 , which exists before the rapid pressure increase.

As $V_f = V_c = V$, (6'), (7') and (8) can be combined and

$$(Q - Q_{leak})/V - \beta^{isoth} \dot{P} + \alpha_f \left(\dot{T}_0 + \frac{\alpha_l T}{\rho_l C_l} \dot{P} \right) = 0 \quad (B.7)$$

where $\beta^{isoth} = \beta_l^{isoth} + \beta_c$ is the cavern compressibility factor. When the cavern is tight ($Q_{leak} = 0$) and the pressure build-up fast enough (\dot{T}_0 can be neglected),

$$Q/V = \beta^{isoth} \dot{P} - \frac{\alpha_l^2 T}{\rho_l C_l} \dot{P} = \beta \dot{P}$$

where β is the adiabatic compressibility factor.

In the case of an oil-filled cavern, typically $\beta^{isoth} = 10^{-3}/\text{MPa}$, $1 - \frac{\alpha_o^2 T}{\beta \rho_o C_o} \approx 0.87$ and $Q \approx 0.87 \beta^{isoth} V \dot{P}$.

Even when the cavern is perfectly tight ($Q_{leak} = 0$) and when the pre-existing temperature rise rate can be disregarded ($\dot{T}_0 \approx 0$, a correct assumption when test duration is short), a significant error (13%) can be made when the ‘‘adiabatic’’ effect is disregarded.

APPENDIX C. Liquid cooling after a rapid temperature increase

C.1. Temperature evolution

Here, we consider the set of equations described in Appendix A:

$$\frac{\partial T_{salt}}{\partial t} = k_{salt} \Delta T_{salt} \quad (C.1)$$

$$T_l(t) = T_{salt} \quad \text{on } \partial\Omega \quad (C.2)$$

$$\rho_l C_l V \dot{T}_l = \int_{\partial\Omega} K_{salt} \frac{\partial T_{salt}}{\partial n} da \quad (C.3)$$

and it is assumed that at time $t = 0$, the rock temperature is zero and the liquid temperature in the cavern is increased by ΔT^0 :

$$T(t=0) = \Delta T^0 \quad \text{and} \quad T_R(t=0, \underline{x}) = 0 \quad (C.4)$$

These conditions exactly fit the case of a rapid pressure increase by ΔP^0 , which generates an instantaneous increase in liquid temperature by $\Delta T^0 = \frac{\alpha_l T}{\rho_l C_l} \Delta P^0$. Evolution of this *additional* temperature change can be described as

$$\Delta T(t) = \Delta T^0 f(t) \quad (C.5)$$

where f is a decreasing function of time such that $f(0) = 1$ and $f(\infty) = 0$. After a very long period of time, the effect of the additional temperature increase vanishes. In fact, $f = f(t)$ is a function of the first thermal characteristic time, $t_c = R^2 / \pi k_{salt} \approx V^{2/3} / 8 k_{salt}$, of the ratio $\chi = \rho_{salt} C_{salt} / \rho_l C_l$ between the volumetric heat capacity of the salt ($\rho_{salt} C_{salt}$), the volumetric heat capacity of the cavern liquid ($\rho_l C_l$) and the cavern shape, or $f = f(t/t_c, \chi, \Omega)$. $f = f(t)$ decreases faster in a smaller cavern and faster in an oil-filled cavern than in a brine-filled cavern. f is such that $f \approx 1/4$ when $t = 2t_c$. $f = f(t)$ can be computed accurately for any given shape of a cavern.

In many cases, pressure in a closed cavern varies continuously, $P = P(t)$. In such cases, temperature evolution can be written as

$$T(t) = T_0(t) + \int_0^t \frac{\alpha_l T_0(\tau)}{\rho_l C_l} \dot{P}(\tau) f(t-\tau) d\tau \quad (C.6)$$

where $T_0(t)$ is the pre-existing brine temperature evolution.

C.2. The case of a spherical cavern

In the case of an idealized spherical cavern, a closed-form solution can be found (Bérest et al., 1979):

$$\left\{ \begin{array}{l} f(t) = \varphi(\xi, v) = W(\xi, v) + W(-\xi, v) \\ W(\xi, v) = \frac{1+\xi}{2\xi} \exp[(1+\xi)^2 v] \operatorname{erfc}[(1+\xi)\sqrt{v}] \\ \xi^2 = \frac{3\chi - 4}{3\chi} \\ v = \frac{9\chi^2 k_{salt} t}{4R^2} = \frac{9\chi^2 t}{4\pi t_c} \end{array} \right. \quad (C.7)$$

This solution can be computed numerically.

For the particular case in which $\chi = 4/3$ (for instance, $\rho_{salt} C_{salt} = 2 \times 10^6 \text{ J/m}^3 \cdot ^\circ\text{C}$ and $\rho_o C_o = 1.5 \times 10^6 \text{ J/m}^3 \cdot ^\circ\text{C}$), the solution takes the following form:

$$\left\{ \begin{array}{l} \xi = 0 \quad v = \frac{4t}{\pi t_c} \\ f(v) = (1+2v) \exp v \operatorname{erfc}\sqrt{v} - 2\sqrt{\frac{v}{\pi}} \\ f'(v) = (3+2v) \exp v \operatorname{erfc}\sqrt{v} - 2\sqrt{\frac{v}{\pi}} - 2\sqrt{\frac{1}{\pi v}} \\ \dot{f}(t) = \frac{4}{\pi t_c} \left[\left(3 + \frac{8t}{\pi t_c} \right) \exp\left(\frac{4t}{\pi t_c}\right) \operatorname{erfc}\sqrt{\frac{4t}{\pi t_c}} - \frac{4}{\pi} \sqrt{\frac{t}{t_c}} - \sqrt{\frac{t_c}{t}} \right] \end{array} \right. \quad (C.8)$$

